IEEE Control Systems Letters paper presented at
2023 American Control Conference (ACC)
San Diego, CA, USA. May 31 - June 2, 2023

Asymptotic Stabilization of Aperiodic Trajectories of a Hybrid-Linear Inverted Pendulum Walking on a Vertically Moving Surface

Amir Iqbal, Sushant Veer, and Yan Gu

Abstract— **This paper presents the analysis and stabilization of a hybrid-linear inverted pendulum (H-LIP) model that describes the essential robot dynamics associated with legged locomotion on a dynamic rigid surface (DRS) with a general vertical motion. The H-LIP model is analytically derived by explicitly capturing the discrete-time foot placement and the continuous-phase dynamics associated with DRS locomotion, and by considering aperiodic DRS motions and variable H-LIP continuous-phase durations. The closed-loop tracking error dynamics of the H-LIP model is then established under a discrete-time feedback footstep control law. The stability of the closed-loop H-LIP error dynamics is analyzed to construct sufficient conditions on the control gains for ensuring the asymptotic error convergence. Simulation results of the proposed H-LIP walking on a vertically moving DRS confirm the proposed control law stabilizes the H-LIP model under various vertical, aperiodic DRS motion profiles and variable H-LIP step durations.**

I. Introduction

Stability is an essential performance measure of legged locomotion. Legged locomotion stability can be loosely defined as the robot's ability to sustain walking without falling over. Previous studies on legged robot planning and control have demonstrated stable legged locomotion on stationary (even or uneven) surfaces [1]–[7]. Particularly, provable stability of legged locomotion has been achieved by explicitly considering the full-order, hybrid, nonlinear dynamics of legged robots and by ensuring the asymptotic stability of the associated hybrid control system [8], [9]. Yet, due to the high complexity [10], [11] of the full-order robot models associated with legged locomotion on a stationary surface, they may not be suitable for serving as the basis of robot planners and controllers. To alleviate the model complexity, various reduce-order robot models have been introduced, among which a widely used one is the linear inverted pendulum (LIP) model.

The LIP model approximates a legged (robot or human) locomotor that walks on a stationary surface as a point mass atop a massless leg [12]. Different variations of the LIP model have been created, including a model that considers the variable height of the point mass above the stationary ground [13], [14]. To explicitly address the hybrid dynamic behaviors of legged locomotors for stationary surface walking, a hybrid LIP (i.e., H-LIP) model [15]–[18] has been introduced, and the asymptotic stability conditions for the H-LIP model have been established based on the theory of hybrid linear time-invariant systems, along with a provably stabilizing, discrete-time footstep controller [15]. Still, the existing LIP models may not be suitable for describing the locomotor dynamics during walking on a dynamic rigid surface (DRS), which is a rigid surface moving in the inertial/world frame, because they do not explicitly account for the time-varying movement of the foot-surface contact point (i.e., support point of the LIP) [19]–[22].

Our recent work has analytically extended the classical LIP model [12] from static to dynamic surfaces and analyzed the stability of the periodic LIP motion under vertical [23], [24] and horizontal surface motions [25], [26]. Yet, it remains unclear how an aperiodic DRS motion affects the stability of the LIP.

This paper focuses on analytically extending the H-LIP model [15] from static surfaces to DRSes that have general (periodic or aperiodic) vertical motions, deriving its stability conditions, synthesizing a discrete-time control law satisfying the conditions, and validating the effectiveness of the proposed work through simulations of aperiodic H-LIP walking on a DRS with general (aperiodic) vertical surface acceleration.

The organization of this paper is as follows. Section II derives the H-LIP model for locomotion on a DRS with a general vertical surface motion. In Sec. III, the derivation of the S2S error dynamics under a discrete-time foot-stepping controller is introduced. Section IV presents the proposed stability analysis of the H-LIP model under variable continuous-phase durations and general vertical DRS movements. In Sec. V, the design of an asymptotically stabilizing footstep controller is presented. Section VI reports simulation results. The paper is concluded in Sec. VII.

Notations. This paper adopts the following notations. $\mathbb{N}$, $\mathbb{R}$, and $\mathbb{R}_+$ denote the complete sets of natural, real, and positive real numbers, respectively. $\mathbb{R}^n$ and $\mathbb{R}^{m\times n}$ ($\forall m,n \in \mathbb{N}$) denote the n-dimensional real vectors and $m \times n$ real matrices, respectively. The notation $|.|$ is the absolute value function of a real scalar. With abuse of notation, we also use $|.|$ to represent the component-wise absolute value function for real vectors and matrices in this study. $\| \, . \, \|$ and $\| \, . \, \|_\infty$ respectively denote the 2-norm and the infinity norm of a vector. For a matrix $\mathbf{A}$, the infinity norm is defined as: $\| \mathbf{A} \|_\infty := \max_i (\sum_j |\mathbf{A}_{ij}|)$ with $\mathbf{A}_{ij}$ the element of $\mathbf{A}$ at the intersection of the i^{th} row and j^{th} column.

II. Hybrid-Linear Inverted Pendulum on a Dynamic Rigid Surface

This section presents the derivation of a hybrid-linear inverted pendulum (H-LIP) model that describes the essential dynamics of legged walking on a dynamic rigid surface (DRS) with a general vertical surface motion.

This work was supported by the National Science Foundation under Grants CMMI-1934280 and CMMI-2046562 and by the Office of Naval Research under Grant N00014-21-1-2582.
A. Iqbal is with the Department of Mechanical Engineering, University of Massachusetts Lowell, Lowell, MA 01854, U.S.A. amir_iqbal@student.uml.edu. S. Veer is with NVIDIA Research, Santa Clara, CA 95051, U.S.A. sveer@nvidia.com. Y. Gu is with the Department of Mechanical Engineering, Purdue University, West Lafayette, IN 4790, U.S.A. yangu@purdue.edu. Corresponding author: Y. Gu.

979-8-3503-2806-6/$31.00 ©2023 AACC

A. Continuous-Phase Dynamics

Legged walking or trotting inherently involves hybrid locomotor behaviors, comprising continuous phases of leg swinging and discrete events of foot touchdowns. Thus, a hybrid model is well suited to describe legged locomotor dynamics. This subsection explains the continuous-phase dynamics of the proposed H-LIP model.

Consider a three-dimensional (3-D) LIP walking on a vertically moving DRS [24], as illustrated in Fig. 1. Under the constant CoM height assumption of the classical LIP model [12], [24], the equations of motion of the LIP model in the x- and y-directions of the wolrd frame are decoupled and share the same form. Thus, we only need to analyze the dynamics in one of the two directions [15]. For brevity, we present the H-LIP model in the x-direction alone.

The selected state vector of the model is $\mathbf{x} := [x_{sc},\ \dot{x}_{sc}]^T$, where x_{sc} and $\dot{x}_{sc}$ are the x-direction position and velocity of the center of mass (CoM) with respect to the support point S in the world frame, respectively.

Within a continuous phase, the LIP dynamics for locomotion on a DRS with a general vertical surface motion is described by the following linear time-varying homogeneous equation [23], [24]:

$$\dot{\mathbf{x}}(t) = \mathbf{A}(t)\mathbf{x}(t), \tag{1}$$

where the expressions of the real matrix $\mathbf{A}(t)$ is given by:

$$\mathbf{A}(t) := \begin{bmatrix} 0 & 1 \\ f(t) & 0 \end{bmatrix}. \tag{2}$$

Here, $f(t) := \frac{(\ddot{z}_{ws}(t)+g)}{z_0}$, with g the magnitude of the gravitational acceleration, z_0 the CoM height above the support point, and $\ddot{z}_{ws}$ the vertical acceleration of the support point S. Note that the explicit time dependence of $\mathbf{A}(t)$ is induced by the vertical surface acceleration $\ddot{z}_{ws}$.

Consider the following practically reasonable assumption on a real-world DRS motion:

(A1) The vertical acceleration $\ddot{z}_{ws}$ of the DRS is bounded as $\ddot{z}_{ws} \in (-g,\ g)$ and is locally Lipschitz on $t \in \mathbb{R}_+$.

Assumption (A1) is automatically satisfied when the unilateral ground-contact constraint is ensured during H-LIP walking on a DRS. The Lipschitz continuity assumption is valid for real-world DRSes such as ships and elevators because they have finite acceleration limits [27], [28].

Let the scalar variable τ_n ($n \in \mathbb{N}$) denote the n^{th} switching instant (i.e., the instant when the swing foot touches down). Let the time duration of the n^{th} continuous phase be $\Delta\tau_n$. Then, $\Delta\tau_n = \tau_{n+1} - \tau_n$. The following assumption on the finite continuous-phase duration is considered:

(A2) The continuous-phase duration $\Delta\tau_n$ of the H-LIP stepping is bounded for any $n \in \mathbb{N}$.

Let $\Delta\tau_m$ and $\Delta\tau_M$ be the lower and upper bounds of $\Delta\tau_n$, respectively. Then, the boundedness of $\Delta\tau_n$ can be expressed as $\Delta\tau_n \in [\Delta\tau_m,\ \Delta\tau_M]$ for any $n \in \mathbb{N}$.

Assumption (A2) is practically reasonable because the desired duration of one continuous phase of H-LIP walking has to be greater than 0 to avoid Zeno behavior and it should have a finite upper bound during real-world mobility tasks.

B. Switching Events

Let $(.)^-$ and $(.)^+$ respectively denote the value of the variable $(.)$ just before and after the switching. At the switching timing (i.e., $t = \tau_n^-$), the support point S of the LIP instantaneously resets its location on the DRS (see Fig. 1). Such a position reset corresponds to the sudden change in the support foot position of a walking robot when its swing foot lands on the ground and becomes the new support foot.

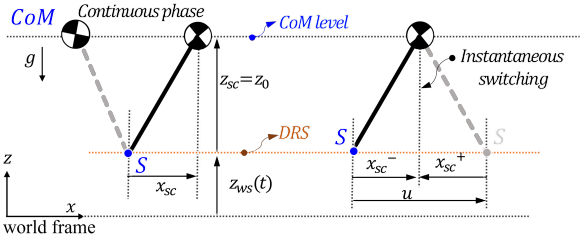

Fig. 1. A 2-D illustration of the H-LIP model walking on a DRS. A 2-D model is adequate for stability analysis because under the assumption of a constant CoM height (i.e., $z_{sc} = z_0$), the 3-D model becomes linear, and the H-LIP dynamics in the x- and y-directions are decoupled and share exactly the same model structure.

This jump in the state $\mathbf{x}$ across the switching event is expressed as [15]:

$$\mathbf{x}^+ = \mathbf{x}^- + \mathbf{B}u. \tag{3}$$

Here, the scalar input variable u is chosen as the step length (denoted as l_x) of the H-LIP in the x-direction (see Fig. 1). The matrix $\mathbf{B}$ is a constant matrix that maps the input u to the state $\mathbf{x}$, and we have $\mathbf{B} = [-1,\ 0]^T$.

From the continuous-phase dynamics in (1) and the reset map in (3), it is clear that the proposed H-LIP model is linear time-varying and can be compactly expressed as:

$$\begin{cases} \dot{\mathbf{x}}(t) = \mathbf{A}(t)\mathbf{x}(t) & \text{if } t \neq \tau_n^-, \\ \mathbf{x}^+ = \mathbf{x}^- + \mathbf{B}u & \text{if } t = \tau_n^-. \end{cases} \tag{4}$$

III. Step-to-Step Error Dynamics under a Discrete-Time Control Law

This section explains a discrete-time stepping controller for the H-LIP model and derives the associated hybrid error dynamics.

A. Hybrid Error Dynamics

To ensure the physical feasibility of the desired H-LIP walking motion, the desired state trajectory of the H-LIP during walking on a DRS is generated to respect the hybrid H-LIP dynamics as described in (4). Thus, the reference state trajectory $\mathbf{x}_r(t)$ should satisfy:

$$\begin{cases} \dot{\mathbf{x}}_r(t) = \mathbf{A}(t)\mathbf{x}_r(t) & \text{if } t \neq \tau_{r,n}^-, \\ \mathbf{x}_r^+ = \mathbf{x}_r^- + \mathbf{B}u_r & \text{if } t = \tau_{r,n}^-, \end{cases} \tag{5}$$

where u_r and $\tau_{r,n}$ respectively denote the values of the input u and the switch timing τ_n associated with the desired state trajectory $\mathbf{x}_r(t)$.

Let $\mathbf{e}$ be the tracking error between the actual and the reference states expressed as:

$$\mathbf{e} := \mathbf{x}(t) - \mathbf{x}_r(t) =: [e,\ \dot{e}]^T. \tag{6}$$

For simplicity of analysis, we consider the following assumption on the switching instants of the H-LIP [15]:

(A3) The switching instants associated with the actual and the reference state trajectories coincide (i.e., $\tau_n = \tau_{r,n}$).

Under assumption (A3), taking the difference between (4) and (5) yields the following hybrid error dynamics:

$$\begin{cases} \dot{\mathbf{e}}(t) = \mathbf{A}(t)\mathbf{e}(t) & \text{if } t \neq \tau_n^-, \\ \mathbf{e}^+ = \mathbf{e}^- + \mathbf{B}(u - u^r) & \text{if } t = \tau_n^-. \end{cases} \tag{7}$$

B. Stepping Controller

Although the H-LIP dynamics during a continuous phase is unactuated and inherently unstable [24], we can directly command the discrete-time dynamics through the control input u. In this study, we design u as the following footstep controller that only acts at the switching instants:

$$u = u_r + \mathbf{K}\mathbf{e}^-, \tag{8}$$

where the feedback gain matrix $\mathbf{K}$ is defined as $\mathbf{K} := [k_1,\ k_2] \in \mathbb{R}^{1\times 2}$, where k_1 and k_2 are scalar real variables to be designed.

By substituting the feedback control law (8) in the hybrid error dynamics in (7), we obtain the overall hybrid closed-loop error dynamics as:

$$\begin{cases} \dot{\mathbf{e}}(t) = \mathbf{A}(t)\mathbf{e}(t) & \text{if } t \neq \tau_n^-, \\ \mathbf{e}^+ = (\mathbf{I} + \mathbf{B}\mathbf{K})\mathbf{e}^- & \text{if } t = \tau_n^-, \end{cases} \tag{9}$$

where $\mathbf{I}$ is an identity matrix with an appropriate dimension.

The objective of the stepping controller in (8) is to asymptotically drive the overall closed-loop error $\mathbf{e}$ to zero; that is, $\lim_{t\to\infty} \mathbf{e}(t) = \mathbf{0}$.

C. Step-to-Step Error Dynamics

We choose to perform the stability analysis for the hybrid error dynamics in (9) based on its step-to-step (S2S) dynamics. The S2S error dynamics is a discrete-time map from the error state just before a switching event to the error state just before the subsequent switching event [15]. Since the S2S dynamics completely characterize the error evolution across a complete hybrid cycle, using it as a basis could simplify the stability analysis.

To derive the S2S model that maps the error state from τ_n^- to τ_{n+1}^- ($\forall n \in \mathbb{N}$), we utilize the hybrid error dynamics in (9) to first apply the state reset map at instant τ_n^- to obtain $\mathbf{e}(\tau_n^+)$, and then to integrate the continuous-phase dynamics from τ_n^+ to τ_{n+1}^-, as introduced next.

By integrating the continuous-phase dynamics of (9) through

$$\int_{\tau_n^+}^{\tau_{n+1}^-} \dot{\mathbf{e}}(t)\, dt = \int_{\tau_n^+}^{\tau_{n+1}^-} \mathbf{A}(t)\mathbf{e}(t) dt,$$

we obtain:

$$\mathbf{e}(\tau_{n+1}^-) = \mathbf{\Phi}(f(t); \tau_{n+1}^-, \tau_n^+)\mathbf{e}(\tau_n^+), \tag{10}$$

where the 2×2 matrix $\mathbf{\Phi}(f(t); \tau_{n+1}^-, \tau_n^+)$ is the state-transition matrix of the n^{th} continuous phase from time instant τ_n^+ to τ_{n+1}^-. The matrix $\mathbf{\Phi}(f(t); \tau_{n+1}^-, \tau_n^+)$ can be computed numerically, e.g., by using the Picard iteration [29].

Substituting the state reset map (9) in (10) yields the S2S dynamics as:

$$\mathbf{e}(\tau_{n+1}^-) = \mathbf{\Phi}(f(t); \tau_{n+1}^-, \tau_n^+)(\mathbf{I} + \mathbf{B}\mathbf{K})\mathbf{e}(\tau_n^-). \tag{11}$$

For brevity, we adopt the following notations: $\mathbf{e}_{n+1}^- := \mathbf{e}(\tau_{n+1}^-)$, $\mathbf{e}_n^- := \mathbf{e}(\tau_n^-)$, and $\mathbf{A}_{d,n} := \mathbf{\Phi}(f(t); \tau_{n+1}^-, \tau_n^+)(\mathbf{I} + \mathbf{B}\mathbf{K})$. Note that $\mathbf{A}_{d,n}$ is essentially the discrete-time S2S mapping matrix for the overall closed-loop error dynamics.

With these notations, the discrete-time S2S error dynamics is compactly expressed as:

$$\mathbf{e}_{n+1}^- = \mathbf{A}_{d,n}\mathbf{e}_n^-. \tag{12}$$

IV. Stability Analysis

This section derives the proposed sufficient stability conditions for the closed-loop H-LIP model based on its S2S error dynamics. These conditions are utilized to guide the design of the foot placement controller for asymptotically stabilizing H-LIP walking on a DRS under a general vertical surface motion and variable continuous-phase durations.

To obtain the stability conditions for variable-duration walking on a DRS with a general vertical surface motion, we cannot directly apply the previous stability conditions for static-surface H-LIP walking [15]. The S2S error dynamics used in the previous work is time-invariant with a constant continuous-phase duration, whereas those of interest to this study are explicitly time-varying with variable-time durations of continuous phases.

We first present the following well-known stability conditions on general discrete-time systems that include the S2S error dynamics in (12), using which we will then derive the sufficient conditions that can be directly used to guide the design of the control gain $\mathbf{K}$. The following theorem is directly adapted from [30].

Theorem 1 (Asymptotic stability conditions for S2S error dynamics): *The discrete-time S2S error dynamics of the H-LIP stepping on a DRS with a general vertical surface motion in* (12) *is uniformly asymptotically stable if and only if there exists a Lyapunov function candidate $V(\mathbf{e}_n)$ satisfying:*

(B1) $V(\mathbf{e}_n) > 0$ $(\forall \mathbf{e}_n \neq \mathbf{0})$ *and* $V(0) = 0$.
(B2) $\alpha_1(\| \mathbf{e}_n \|) \leq V(\mathbf{e}_n) \leq \alpha_2(\| \mathbf{e}_n \|)$.
(B3) $\Delta V(\mathbf{e}_n^-) := V(\mathbf{e}_{n+1}^-) - V(\mathbf{e}_n^-) \leq -\alpha_3(\| \mathbf{e}_n^- \|)$.

Here $\alpha_i(.)$ $(i \in \{1,2,3\})$ is a κ_∞ function; that is, $\alpha_i(.) : \mathbb{R}_+ \mapsto \mathbb{R}_+$ is continuous and strictly increasing with $\alpha_i(0) = 0$ and $\alpha_i(\infty) \to \infty$.

To obtain sufficient conditions on the control gain $\mathbf{K}$ based on the general stability conditions (B1)-(B3), we choose the Lyapunov function candidate as:

$$V(\mathbf{e}) := \frac{1}{2}\mathbf{e}^T\mathbf{e} = \frac{1}{2}\| \mathbf{e} \|^2. \tag{13}$$

Clearly, the function $V(\mathbf{e})$ in (13) is positive definite and meets conditions (B1) and (B2). To ensure that $V(\mathbf{e})$ also satisfies condition (B3) under the proposed control law, we analyze its evolution under the S2S error dynamics in (12), as explained in the rest of this section.

A. Boundedness of Function $f(t)$

From the expression of $f(t)$ in (2) and assumption (A2), we know that $f(t)$ is a positive, bounded function on $t \in \mathbb{R}^+$. Let the positive constants f_m and f_M respectively denote the lower and upper bounds of $f(t)$ on $t \in \mathbb{R}^+$; e.g., $f_m := \inf_{t\in\mathbb{R}^+} f(t)$ and $f_M := \sup_{t\in\mathbb{R}^+} f(t)$. Then, $0 < f_m \leq f(t) \leq f_M$ on $t \in \mathbb{R}^+$.

Lemma 1 (Boundedness of continuous-phase solutions): *Consider the linear, time-varying, continuous-time system $\ddot{\tilde{e}} - f(t)\tilde{e} = 0$ along with the following two systems:*

$$\ddot{e}_m - f_m e_m = 0 \text{ and} \tag{14}$$

$$\ddot{e}_M - f_M e_M = 0. \tag{15}$$

Under the same initial condition for these three systems,

$$|e_m(t)| \leq |\tilde{e}(t)| \leq |e_M(t)|$$

holds for any $t \in \mathbb{R}_+$.

As Lemma 1 is directly adapted from Sec. 2 in [31], its proof is omitted for space consideration.

Let $\mathbf{\Phi}_m$ and $\mathbf{\Phi}_M$ respectively denote the state-transition matrices associated with (14) and (15). By Lemma 1, we utilize the state evolutions of (14) and (15) to obtain the following boundedness of $|\mathbf{e}_{n+1}^-|$ under the initial condition $\mathbf{e}_n^+$:

$$|\mathbf{\Phi}_m(f_m;\tau_{n+1}^-,\tau_n^+)\mathbf{e}_n^+| \leq |\mathbf{e}_{n+1}^-| \leq |\mathbf{\Phi}_M(f_M;\tau_{n+1}^-,\tau_n^+)\mathbf{e}_n^+| \quad (16)$$

Since (14) and (15) are linear time-invariant systems, we have

$$\begin{aligned}&\mathbf{\Phi}_m(f_m;\tau_{n+1}^-,\tau_n^+) = \mathbf{\Phi}_m(f_m;\Delta\tau_n,0) \text{ and}\\ &\mathbf{\Phi}_M(f_M;\tau_{n+1}^-,\tau_n^+) = \mathbf{\Phi}_M(f_M;\Delta\tau_n,0).\end{aligned} \quad (17)$$

Also, recall $\mathbf{e}_n^+ = (\mathbf{I}+\mathbf{BK})\mathbf{e}_n^-$. Then, the inequality in (16) becomes:

$$\begin{aligned}|\mathbf{\Phi}_m(f_m;\Delta\tau_n,0)(\mathbf{I}+\mathbf{BK})\mathbf{e}_n^-| &\leq |\mathbf{e}_{n+1}^-|\\ &\leq |\mathbf{\Phi}_M(f_M;\Delta\tau_n,0)(\mathbf{I}+\mathbf{BK})\mathbf{e}_n^-|\end{aligned} \quad (18)$$

Define

$$\begin{aligned}&\underline{\mathbf{A}}_{d,n} := \mathbf{\Phi}_m(f_m;\Delta\tau_n,0)(\mathbf{I}+\mathbf{BK}) \text{ and}\\ &\overline{\mathbf{A}}_{d,n} := \mathbf{\Phi}_M(f_M;\Delta\tau_n,0)(\mathbf{I}+\mathbf{BK}).\end{aligned} \quad (19)$$

With these notations, (18) is rewritten as:

$$|\underline{\mathbf{A}}_{d,n}\mathbf{e}_n^-| \leq |\mathbf{e}_{n+1}^-| \leq |\overline{\mathbf{A}}_{d,n}\mathbf{e}_n^-|. \quad (20)$$

The right-hand side of this inequality is utilized for proving the following sufficient condition of asymptotic stability in Theorem 2.

B. Sufficient Stability Conditions

Theorem 2 (Sufficient closed-loop stability conditions): *Consider the following condition:*

(C1) There exists a feedback gain $\mathbf{K}$ *for the stepping controller in* (8) *such that*

$$a_d := \| \overline{\mathbf{A}}_{d,n} \|_\infty < 1 \quad (21)$$

holds for any $f \in [f_m, f_M]$, $n \in \mathbb{N}$, *and* $\Delta\tau_n \in [\Delta\tau_m,\ \Delta\tau_M]$.

Then, the overall closed-loop S2S error dynamics in (12) *is asymptotically stable.*

Proof: Using the right-hand side of the inequality in (20) and the properties of component-wise absolute value function $|.|$, we have:

$$|\mathbf{e}_{n+1}^-| \leq |\overline{\mathbf{A}}_{d,n}\mathbf{e}_n^-| \leq |\overline{\mathbf{A}}_{d,n}||\mathbf{e}_n^-|. \quad (22)$$

Note that by the definition of the component-wise absolute value function $|.|$ explained in Sec. I-C, $|\overline{\mathbf{A}}_{d,n}|$ is a real matrix with all elements positive while $|\mathbf{e}_n^-|$ is a real vector with all elements positive.

Upon writing the error vector relation in (22) as a quadratic form and utilizing the properties of induced norms, we obtain:

$$\begin{aligned}(\mathbf{e}_{n+1}^-)^T\mathbf{e}_{n+1}^- &\leq (|\overline{\mathbf{A}}_{d,n}||\mathbf{e}_n^-|)^T|\overline{\mathbf{A}}_{d,n}||\mathbf{e}_n^-|\\ &= \| (|\overline{\mathbf{A}}_{d,n}||\mathbf{e}_n^-|) \|^2\\ &\leq (\| \overline{\mathbf{A}}_{d,n} \|_\infty \| \mathbf{e}_n^- \|)^2 = a_d^2 \| \mathbf{e}_n^- \|^2.\end{aligned} \quad (23)$$

We are now ready to examine the upper bound of $\Delta V(\mathbf{e}_n^-)$:

$$\begin{aligned}\Delta V(\mathbf{e}_n^-) = V(\mathbf{e}_{n+1}^-) - V(\mathbf{e}_n^-) &= \frac{1}{2}\| \mathbf{e}_{n+1}^- \|^2 - \frac{1}{2}\| \mathbf{e}_n^- \|^2\\ &\leq \frac{1}{2}a_d^2 \| \mathbf{e}_n^- \|^2 - \frac{1}{2}\| \mathbf{e}_n^- \|^2 =: -\gamma \| \mathbf{e}_n^- \|^2,\end{aligned} \quad (24)$$

where $\gamma := \frac{1}{2}(1-a_d^2) \in (0,\ \frac{1}{2})$.

From (24), it is clear that $\Delta V(\mathbf{e}_n^-)$ satisfies condition (B3) of Theorem 1. Thus, if condition (C1) is met, then the Lyapunov function candidate in (13) satisfies all the conditions in Theorem 1, which concludes the proof. ■

V. Asymptotically Stabilizing Footstep Controller Design

This section presents a systematic way to utilize the proposed stability conditions to design feedback gains that asymptotically stabilize the linear, hybrid, time-varying H-LIP error dynamics.

To guarantee the asymptotic stability of the H-LIP based on Theorem 2, we design the stepping control gain $\mathbf{K}$ in (8) such that $\| \mathbf{A}_{d,n} \| < 1$ for any $f(t) \in [f_m, f_M]$ and $n \in \mathbb{N}$.

Theorem 3 (Sufficient stability conditions on control gain): The feedback stepping-controller gain $\mathbf{K}$ (i.e., k_1 and k_2) ensures the asymptotic closed-loop stability of the H-LIP error system in Eq. (9) for the given foot-stepping duration $\Delta\tau_n$ and the known constant f_M, if the controller gains k_1 and k_2 satisfy the following inequalities for any $n \in \mathbb{N}$:

$$\begin{aligned}&2\left|\cosh(\sqrt{f_M}\Delta\tau_n)(1-k_1)\right| < 1,\\ &2\left|\frac{1}{\sqrt{f_M}}\sinh(\sqrt{f_M}\Delta\tau_n) - \cosh(\sqrt{f_M}\Delta\tau_n)k_2\right| < 1,\\ &2\left|\sqrt{f_M}\sinh(\sqrt{f_M}\Delta\tau_n)(1-k_1)\right| < 1, \text{ and}\\ &2\left|\cosh(\sqrt{f_M}\Delta\tau_n) - \sqrt{f_M}\sinh(\sqrt{f_M}\Delta\tau_n)k_2\right| < 1.\end{aligned} \quad (25)$$

Proof: From (19) and Theorem 2, we know the controller gain $\mathbf{K}$ needs to meet the following condition to ensure the system stability:

$$\| \overline{\mathbf{A}}_{d,n} \|_\infty = \| \mathbf{\Phi}_M(f_M;\Delta\tau_n,0)(\mathbf{I}+\mathbf{BK}) \|_\infty < 1. \quad (26)$$

Recall that the linear time-invariant system in (15) can be rewritten as:

$$\begin{bmatrix}\dot{e}_M\\ \ddot{e}_M\end{bmatrix} = \mathbf{A}_M \begin{bmatrix}e_M\\ \dot{e}_M\end{bmatrix},$$

where $A_M := \begin{bmatrix}0 & 1\\ f_M & 0\end{bmatrix}$.

Since $\mathbf{\Phi}_M$ is the state-transition matrix of the continuous-time linear time-invariant system in (15), we can express $\mathbf{\Phi}_M$ as:

$$\mathbf{\Phi}_M(f_M;t,0) := e^{A_M t} = \begin{bmatrix}\cosh\sqrt{f_M}t & \frac{1}{\sqrt{f_M}}\sinh\sqrt{f_M}t\\ \sqrt{f_M}\sinh\sqrt{f_M}\Delta\tau_n & \cosh\sqrt{f_M}t\end{bmatrix}.$$

With the expressions of the state-transition matrix $\mathbf{\Phi}_M$, the

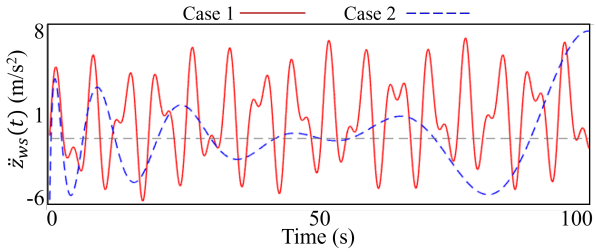

Fig. 2. General aperiodic vertical acceleration profiles of the DRS.

mapping matrix $\mathbf{B}$, and the gain matrix $\mathbf{K}$, we obtain:

$$\left|\boldsymbol{\Phi}_M(f_M;\Delta\tau_n,0)(\mathbf{I}+\mathbf{BK})\right| = \left|\begin{bmatrix}(1-k_1)\boldsymbol{\Phi}_{M,11} & \boldsymbol{\Phi}_{M,12}-k_2\boldsymbol{\Phi}_{M,11}\\ (1-k_1)\boldsymbol{\Phi}_{M,21} & \boldsymbol{\Phi}_{M,22}-k_2\boldsymbol{\Phi}_{M,21}\end{bmatrix}\right|, \tag{27}$$

where $\boldsymbol{\Phi}_{M,ij}$ denotes the element at the i^{th} row and j^{th} column of the state-transition matrix $\boldsymbol{\Phi}_M(f_M;\Delta\tau_n,0)$, and

$$\begin{aligned}&\boldsymbol{\Phi}_{M,11}=\cosh(\sqrt{f_M}\Delta\tau_n),\ \boldsymbol{\Phi}_{M,12}=\frac{1}{\sqrt{f_M}}\sinh(\sqrt{f_M}\Delta\tau_n),\\ &\boldsymbol{\Phi}_{M,21}=\sqrt{f_M}\sinh(\sqrt{f_M}\Delta\tau_n),\ \boldsymbol{\Phi}_{M,22}=\cosh(\sqrt{f_M}\Delta\tau_n).\end{aligned} \tag{28}$$

With the expressions of $\boldsymbol{\Phi}_{M,ij}$, the conditions in (25) are equivalent to:

$$\begin{aligned}&2|\boldsymbol{\Phi}_{M,11}(1-k_1)|<1,\ 2|\boldsymbol{\Phi}_{M,12}-\boldsymbol{\Phi}_{M,11}k_2|<1,\\ &2|\boldsymbol{\Phi}_{M,21}(1-k_1)|<1,\ \text{and}\ 2|\boldsymbol{\Phi}_{M,22}-\boldsymbol{\Phi}_{M,21}k_2|<1\end{aligned} \tag{29}$$

for any $n\in\mathbb{N}$.

Under these conditions, we can obtain

$$\begin{aligned}&|\boldsymbol{\Phi}_{M,11}(1-k_1)|+|\boldsymbol{\Phi}_{M,12}-\boldsymbol{\Phi}_{M,11}k_2|<1\ \text{and}\\ &|\boldsymbol{\Phi}_{M,21}(1-k_1)|+|\boldsymbol{\Phi}_{M,22}-\boldsymbol{\Phi}_{M,21}k_2|<1\end{aligned} \tag{30}$$

for any $n\in\mathbb{N}$. Then, by the definition of the infinity norm $\|\,.\,\|_\infty$, we know $\|\,\mathbf{A}_{d,n}\,\|_\infty := \max(|\boldsymbol{\Phi}_{M,11}(1-k_1)|+|\boldsymbol{\Phi}_{M,12}-\boldsymbol{\Phi}_{M,11}k_2|,\ |\boldsymbol{\Phi}_{M,21}(1-k_1)|+|\boldsymbol{\Phi}_{M,22}-\boldsymbol{\Phi}_{M,21}k_2|)<1$.

■

We compute control gains k_1 and k_2 for a given set of parameters f_M and $\Delta\tau_n$ such that they satisfy (25). Theorem 3 guarantees that these gains asymptotically stabilize the closed-loop H-LIP error dynamics.

VI. Simulations

This section presents the validation results for the proposed stability conditions under two different cases of aperiodic vertical surface motion.

A. Simulation Setup

1) DRS motions: We consider the following two general vertical acceleration profiles for simulation validation:

(a) Case 1: The vertical acceleration of the DRS is composed of polynomial and sinusoidal functions, and is given as:

$$\ddot{z}_{ws}(t) := 3\sin t + 2\sin\sqrt{3}t + \frac{t^2+1}{t^2+20t+5}\ (\text{m/s}^2). \tag{31}$$

(b) Case 2: The vertical acceleration is given as:

$$\ddot{z}_{ws}(t) := (e^{0.022t}-5e^{-0.01t})\cos\sqrt{10t}\ (\text{m/s}^2). \tag{32}$$

Figure 2 displays the vertical DRS acceleration profiles of Cases 1 and 2.

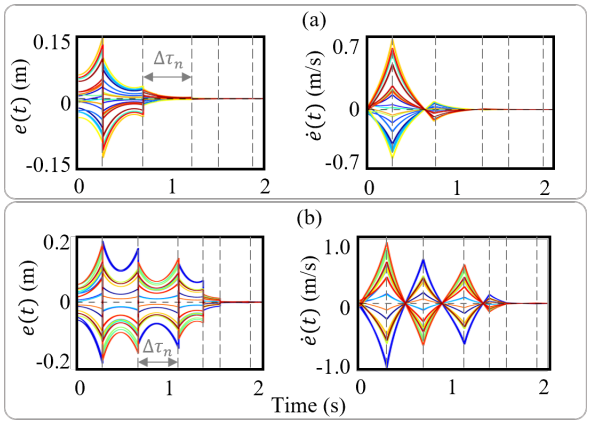

Fig. 3. The error state convergence under the proposed foot-stepping controller for two cases of vertical surface acceleration: (a) Case 1 and (b) Case 2. The switching instants of the H-LIP are marked by vertical lines on the time axis, and the duration of the n^{th} step is denoted by $\Delta\tau_n$.

Note that the surface acceleration profiles in both cases cover the common range of the vertical accelerations of real-world DRSes such as ships whose vertical acceleration is typically less than 3 m/s^2 in magnitude [27], [28].

2) User-defined parameters: The user-defined parameters for each case are given in Table I, which include the CoM height z_0, gait duration $\Delta\tau_n$, walking speed, and step length $l_{r,x}$. Note that we utilize the DRS vertical acceleration profile and user-defined parameter z_0 to determine the range of $f(t)$.

TABLE I
User-defined desired parameters of the H-LIP.

Parameters	Case 1	Case 2
H-LIP CoM height z_0 (cm)	30	30
Gait duration $\Delta\tau_n$ (s)	[0.15, 0.5]	[0.15, 0.5]
Walking speed (cm/s)	[20, 67]	[16, 54]
Step length $l_{r,x}$ (cm)	10	8

3) Initial conditions: The presented simulation results for both cases correspond to twenty random initial conditions satisfying $|e|\le 5$ cm and $|\dot{e}|\le 5$ cm/s.

4) Controller gains: With the user-specified range of step duration $\Delta\tau_n$ and DRS acceleration profiles in both Cases 1 and 2, we observe that there exists a finite range of gains that fulfill the sufficient stability conditions in (25), and the computed gains for Cases 1 and 2 are $\mathbf{K}=[1,\ 0.18]$ and $\mathbf{K}=[1,\ 0.17]$, respectively. The analysis in Sec. V guarantees that for any given set of parameters f_M and $\Delta\tau_n$, these gains asymptotically stabilize the H-LIP closed-loop error dynamics.

B. Results

With the gain setting of Case 1, the evolution of the closed-loop error state $[e,\ \dot{e}]^T$ for the first two seconds is shown in Fig. 3 (a).The stepping controller asymptotically stabilizes the H-LIP error dynamics for all twenty initial conditions. The initial error converges to approximately zero in less than two seconds.

Figure 3 (b) illustrates the asymptotic convergence of the closed-loop error state for the initial two seconds of Case 2. Yet, it takes a relatively longer time than Case 1 to converge to zero. The slower convergence rate in Case 2 may be attributed to the selected constant gains.

In both simulation cases, the H-LIP model behaves as an open-loop unstable system until the first foot touchdown, resulting in a significant increase in error during the initial continuous phase. However, when a walking step is taken, the feedback stepping controller is activated, leading to a gradual decrease in error until it asymptotically reaches zero.

VII. Conclusion

This paper has introduced a hybrid-linear inverted pendulum (H-LIP) model that can be used to capture the essential robot dynamics associated with legged walking on a dynamic rigid surface (DRS) under a general (periodic or aperiodic) vertical surface motion. Based on the H-LIP model and its error state dynamics, a discrete-time footstep feedback control law was introduced, and the asymptotic stability of the resulting closed-loop tracking error dynamics was analyzed under variable continuous-phase durations and aperiodic vertical DRS accelerations. The effectiveness of the proposed control law in asymptotically stabilizing the H-LIP error dynamics was validated under various significant aperiodic DRS motions.

Our future work will build upon the results from this study to investigate the stabilization of real-world legged robot locomotion under a general DRS motion profile. We will extend the proposed stability conditions by relaxing the assumption that the desired and actual impact timings should coincide, and develop a systematic method to design the footstep controller gains.

References

[1] M. Hutter, C. Gehring, D. Jud, A. Lauber, C. D. Bellicoso, V. Tsounis, J. Hwangbo, K. Bodie, P. Fankhauser, M. Bloesch, *et al.*, "ANYmal-a highly mobile and dynamic quadrupedal robot," in *Proc. IEEE/RSJ Int. Conf. Intell. Robot. Syst. (IROS)*, pp. 38–44, 2016.

[2] Z. Zhang, J. Yan, X. Kong, G. Zai, and Y. T. Liu, "Efficient motion planning based on kinodynamic model for quadruped robots following persons in confined spaces," *IEEE/ASME Trans. Mechatron.*, 2021.

[3] A. W. Winkler, C. Mastalli, I. Havoutis, M. Focchi, D. G. Caldwell, and C. Semini, "Planning and execution of dynamic whole-body locomotion for a hydraulic quadruped on challenging terrain," in *Proc. IEEE Int. Conf. Rob. Autom.*, pp. 5148–5154, 2015.

[4] S. Kuindersma, R. Deits, M. Fallon, A. Valenzuela, H. Dai, F. Permenter, T. Koolen, P. Marion, and R. Tedrake, "Optimization-based locomotion planning, estimation, and control design for the Atlas humanoid robot," *Auton. Robots*, vol. 40, no. 3, pp. 429–455, 2016.

[5] G. Bledt, M. J. Powell, B. Katz, J. Di Carlo, P. M. Wensing, and S. Kim, "MIT Cheetah 3: design and control of a robust, dynamic quadruped robot," in *Proc. IEEE/RSJ Int. Conf. Intell. Robot. Syst.*, pp. 2245–2252, 2018.

[6] Y. Gu, B. Yao, and C. S. G. Lee, "Exponential stabilization of fully actuated planar bipedal robotic walking with global position tracking capabilities," *J. Dyn. Syst. Meas. Contr.*, vol. 140, no. 5, 2018.

[7] Y. Gao and Y. Gu, "Global-position tracking control of multi-domain planar bipedal robotic walking," in *Proc. ASME Dyn. Syst. Contr. Conf.*, 2019.

[8] J. W. Grizzle, G. Abba, and F. Plestan, "Asymptotically stable walking for biped robots: Analysis via systems with impulse effects," *IEEE Trans. Autom. Contr.*, vol. 46, no. 1, pp. 51–64, 2001.

[9] S. Veer, I. Poulakakis, *et al.*, "Input-to-state stability of periodic orbits of systems with impulse effects via poincaré analysis," *IEEE Trans. Autom. Contr.*, vol. 64, no. 11, pp. 4583–4598, 2019.

[10] Y. Gao and Y. Gu, "Global-position tracking control of multi-domain planar bipedal robotic walking," in *Proc. ASME Dyn. Syst. Contr. Conf.*, 2019.

[11] M. S. Motahar, S. Veer, and I. Poulakakis, "Composing limit cycles for motion planning of 3d bipedal walkers," in *Proc. IEEE Conf. Dec. Contr.*, pp. 6368–6374, 2016.

[12] S. Kajita, F. Kanehiro, K. Kaneko, K. Yokoi, and H. Hirukawa, "The 3d linear inverted pendulum mode: A simple modeling for a biped walking pattern generation," in *Proc. IEEE Int. Conf. Intell. Robot. Sys.*, vol. 1, pp. 239–246, 2001.

[13] S. Caron, A. Escande, L. Lanari, and B. Mallein, "Capturability-based pattern generation for walking with variable height," *IEEE Trans. Robot.*, vol. 36, no. 2, pp. 517–536, 2019.

[14] S. Caron, "Biped stabilization by linear feedback of the variable-height inverted pendulum model," in *Proc. IEEE Int. Conf. Robot. Autom.*, pp. 9782–9788, 2020.

[15] X. Xiong and A. Ames, "3D underactuated bipedal walking via h-lip based gait synthesis and stepping stabilization," *arXiv preprint arXiv:2101.09588*, 2021.

[16] Y. Gong and J. Grizzle, "Angular momentum about the contact point for control of bipedal locomotion: Validation in a LIP-based controller," *arXiv preprint arXiv:2008.10763*, 2020.

[17] M. Dai, X. Xiong, and A. Ames, "Bipedal walking on constrained footholds: Momentum regulation via vertical com control," in *Proc. IEEE Int. Conf. Rob. Autom*, pp. 10435–10441, 2022.

[18] V. Paredes and A. Hereid, "Resolved motion control for 3D underactuated bipedal walking using linear inverted pendulum dynamics and neural adaptation," *arXiv preprint arXiv:2208.01786*, 2022.

[19] A. Iqbal, Y. Gao, and Y. Gu, "Provably stabilizing controllers for quadrupedal robot locomotion on dynamic rigid platforms," *IEEE/ASME Trans. Mechatron.*, vol. 25, no. 4, pp. 2035–2044, 2020.

[20] A. Iqbal, Z. Mao, and Y. Gu, "Modeling, analysis, and control of slip running on dynamic platforms," *ASME Lett. Dyn. Sys. Contr.*, vol. 1, no. 2, 2021.

[21] Y. Gao, C. Yuan, and Y. Gu, "Invariant extended kalman filtering for hybrid models of bipedal robot walking," in *Proc. IFAC Mod. Est. Contr. Conf.*, vol. 54, pp. 290–297, 2021.

[22] Y. Gao, C. Yuan, and Y. Gu, "Invariant filtering for legged humanoid locomotion on dynamic rigid surfaces," *IEEE Trans. Mechatron.*, 2022, in press.

[23] A. Iqbal and Y. Gu, "Extended capture point and optimization-based control for quadrupedal robot walking on dynamic rigid surfaces," in *Proc. IFAC Mod. Est. Contr. Conf.*, vol. 54, pp. 72–77, 2021.

[24] A. Iqbal, S. Veer, and Y. Gu, "DRS-LIP: Linear inverted pendulum model for legged locomotion on dynamic rigid surfaces," *arXiv preprint arXiv:2202.00151*, 2022.

[25] Y. Gao, V. Cauna, A. Hereid, and Y. Gu, "Exponential stabilization of periodic LIP walking on a horizontally moving surface," *Dynamic Walking*, 2022.

[26] Y. Gao, Y. Gong, V. Paredes, A. Hereid, and Y. Gu, "Time-varying ALIP model and robust foot-placement control for underactuated bipedal robot walking on a swaying rigid surface," *arXiv preprint arXiv:2210.13371*, 2022.

[27] E. A. Tannuri, J. V. Sparano, A. N. Simos, and J. J. Da Cruz, "Estimating directional wave spectrum based on stationary ship motion measurements," *App. Ocean Res.*, vol. 25, no. 5, pp. 243–261, 2003.

[28] L. Bergdahl, "Wave-induced loads and ship motions," tech. rep., Chalmers University of Technology, 2009.

[29] M. Vidyasagar, *Nonlinear systems analysis*. SIAM, 2002.

[30] J. Daafouz and J. Bernussou, "Parameter dependent lyapunov functions for discrete time systems with time varying parametric uncertainties," *Syst. Contr. Lett.*, vol. 43, no. 5, pp. 355–359, 2001.

[31] A. McNabb, "Comparison theorems for differential equations," *J. Math. Anal. Appl.*, vol. 119, no. 1-2, pp. 417–428, 1986.